

2
3 **Functionally graded tungsten/EUROFER coating for DEMO First Wall:**

4 **From laboratory to industrial production**

5 Thilo Grammes^{1*}, Thomas Emmerich¹, Dandan Qu^{1,2}, Oliver Heinze¹, Robert Vaßen³, Jarir Aktaa¹

6 ¹Karlsruhe Institute of Technology (KIT), Institute for Applied Materials, Hermann-von-Helmholtz-Platz 1, 76344 Eggenstein-
7 Leopoldshafen, Germany

8 ²Now at: Wide Range Flight Engineering Science and Application Center, Institute of Mechanics, Chinese Academy of Sciences,
9 Beijing 100190, China

10 ³Forschungszentrum Jülich, Institute of Energy and Climate Research (IEK-1), Wilhelm-Johnen-Straße, 52428 Jülich, Germany

11 *Corresponding Author: Thilo Grammes (thilo.grammes@kit.edu)

12 **Abstract**

13 The First Wall is a crucial component for the realisation of DEMO. It has to protect the tritium breeding
14 blanket from erosion by high-energy particles while letting neutrons pass to enable breeding of tritium fuel.
15 Furthermore, the First Wall needs to pass incoming heat in the MW/m² range to a cooling system for
16 conversion to electric power. These requirements sum up to one of the harshest environments imaginable
17 for a man-made material. Structural steel components alone cannot withstand these conditions. Tungsten
18 is a viable armour material for the First Wall because of its low sputtering yield, high melting point, low
19 activation and good thermal conductivity. It is not suitable though as bulk structural material because of its
20 brittleness. Instead, the DEMO design foresees a First Wall of reduced-activation EUROFER steel, covered
21 with a protective layer of tungsten. Direct tungsten-steel joints suffer from failure during processing or
22 operation because of the thermal expansion mismatch between the two materials. This is solved by
23 application of a functionally graded material as intermediate layer between steel and tungsten. Such
24 coatings made of both tungsten and EUROFER, with a compositional gradient, have been produced with
25 vacuum plasma spray technology. This technology enables manufacturing of the required millimetre-thick
26 coatings and is suitable for upscaling. The development was supported by thermo-mechanical finite element
27 simulations of load scenarios during processing and in-vessel service. Driven by promising results of high
28 heat flux tests on larger, coated mock-ups the technology was transferred to industry for upscaling. Plates
29 with a record size of 500x250 mm² and cooling channels were successfully coated. This contribution
30 presents an overview of the development process, covers the latest results of ongoing research on the
31 coating of curved First Wall structures and addresses future requirements.

32 **Keywords:** plasma-facing component, functionally graded material (FGM), First Wall, finite element
33 simulation, tungsten, EUROFER.

34 **1. Introduction**

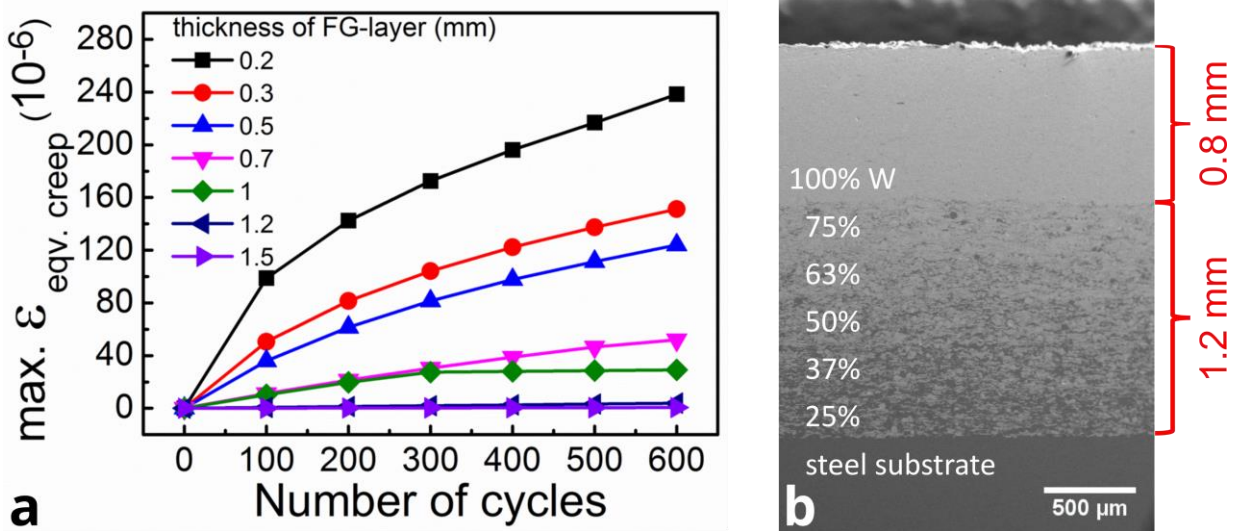
35 The European Demonstration Power Plant (DEMO) is a future fusion energy facility that requires self-
36 sufficiency in terms of tritium fuel [1,2]. Following the helium-cooled pebble bed design (HCPB) as a possible
37 solution for tritium generation [3], the reactor's plasma will be surrounded by tritium breeding modules which
38 are covered by the First Wall (FW). The First Wall consists of plates of reduced-activation ferritic martensitic
39 steel, e.g. EUROFER [4], and contains cooling channels connected to a helium cycle for heat transfer and
40 energy harvesting [5]. During reactor operation the First Wall will be exposed to cyclic thermal load in the
41 MW/m² range as well as bombardment by high-energy particles from the fusion plasma. The unprotected
42 steel would suffer mechanical softening as well as sputtering erosion under such conditions [6,7]. Therefore,
43 a protective 2 mm thick coating of tungsten is foreseen for the First Wall [7,8]. However, the lasting
44 application of such coatings is impeded by the high thermal expansion mismatch between tungsten and
45 steel [6,9].

46 This issue can be solved by creating a smooth transition between the material properties by applying a
47 functionally graded material (FGM) between steel and tungsten. Over the past years such tungsten coatings
48 with FGM interlayers have been developed in a collaboration between Karlsruhe Institute of Technology
49 (KIT, Karlsruhe, Germany) and Forschungszentrum Jülich (FZJ, Jülich, Germany) by applying a multilayer
50 system onto steel substrates [6,10,11]. Each interlayer of this multilayer system consists of mixed
51 EUROFER steel and tungsten. The tungsten content is gradually increased from the steel substrate towards
52 a 100% tungsten top coating. Out of various potential FGM production techniques vacuum plasma spraying
53 (VPS) has been identified as suitable for coating of the First Wall [10–13,13–16]. VPS readily achieves the
54 desired material gradient at sufficient microstructural quality, is suitable for the high coating thickness
55 (2 mm) specified in DEMO, avoids excessive oxidation of the coating and in general thermal spraying bears
56 potential for process upscaling to large coated areas [11,12,14,16]. This contribution aims to provide an
57 overview over past and present development steps of these functionally graded W/EUROFER protective
58 coatings for the First Wall and addresses future challenges.

59 **2. Review of previous development steps**

60 In order to assess feasibility and to find good parameters for both processing and FGM design, early test
61 FGM coatings were created on small EUROFER blocks (100×100×18 mm³) [11,14,17], or on similarly sized
62 blocks of the tungsten alloy WL10, the latter building on similar developments for divertor joints [12]. Among
63 the parameters to be optimised were the size distribution of the feed stock powders, current of spray gun,
64 stand-off distance, chamber pressure, velocity of the spray gun, but also the number and composition of the
65 interlayers and the thickness of the FGM [11,12,14,17,18]. The quality of these coatings was assessed in
66 view of microstructure, achieved gradient in chemical composition as well as mechanical hardness [12,14],
67 by quantifying the residual stresses in the coating [11], and the interface toughness between coating and
68 substrate [18,19], the thermal fatigue behaviour and thermal diffusivity of the coating [16,20] and ultimately
69 by investigating their resistance against transient heat loads that simulate edge-localised modes [17,21].

70 With such a multitude of parameters to be optimised both in processing and coating design, a purely
 71 experimental approach would be excessively expensive and time-consuming. Therefore, the development
 72 of these FGMs was accompanied by finite element simulations in order to predict optimum parameters, e.g.
 73 for the number of interlayers, the type of chemical gradient (linear/quadratic over thickness) and the
 74 thickness of the FGM [6,22]. Optimised parameters were experimentally investigated for their suitability
 75 [12,14,19]. As an example, the finding of an optimum thickness will be briefly discussed here. A good
 76 tungsten coating requires a certain minimum thickness of FGM interlayer to achieve long-lasting
 77 performance under reactor conditions, because the above-mentioned mismatch in thermal expansion
 78 coefficient between tungsten and steel needs to be mitigated. On the other hand, simulations on the tritium
 79 self-sufficiency of future fusion reactors, covering either neutronics [23] or tritium retention in wall
 80 components [1] both call for a tungsten coating to be as thin as possible in order to achieve a higher tritium
 81 breeding ratio and to trap less tritium in the wall. Indeed the predictions on trapped tritium have to be seen
 82 as a major challenge to the realisation of fusion energy, with predicted tritium retention losses being as high
 83 as half a kilogram [1]. However, these simulations usually assume a 2mm thick coating of dense, 100%
 84 tungsten. The tritium retention study reported in [1] compared this with a functionally graded coating as
 85 presented here, finding comparably high retention, but assuming pure EUROFER properties for the FGM in
 86 absence of tritium permeation data. The FGM coatings investigated here contain a fraction of steel and a
 87 minor level of porosity [14,24] which may substantially influence the tritium retention characteristics. A future
 88 experimental characterisation of the hydrogen retention of these coatings is therefore of major interest.

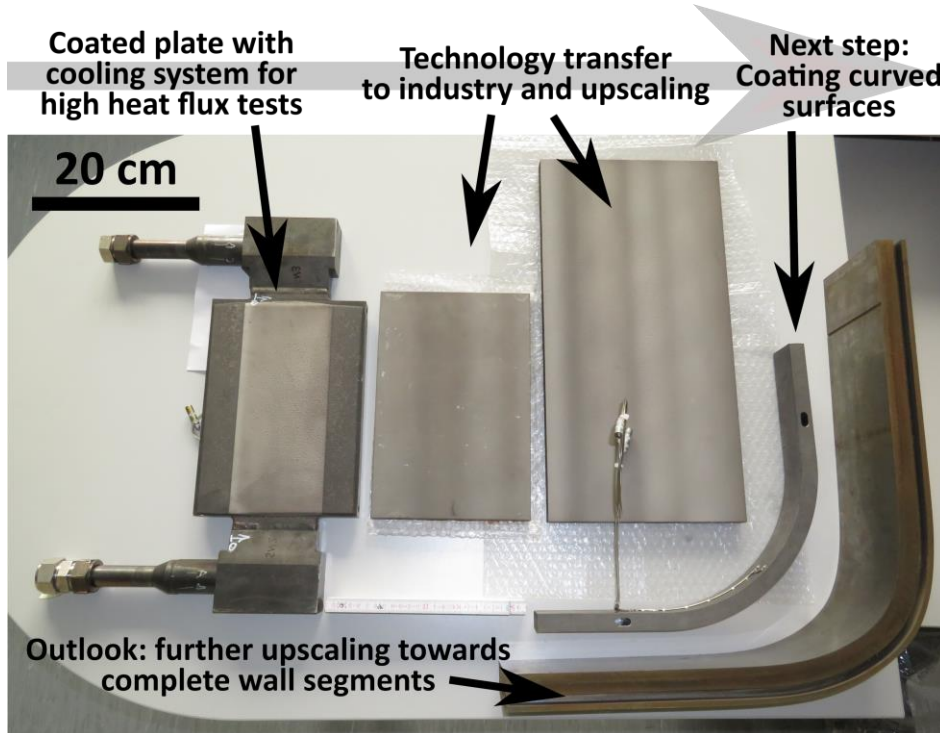


89 **a**
 90 *Figure 1. (a) Maximum equivalent creep strain in the steel substrate for varying coating thickness, over several hundred*
 91 *simulated operational cycles. Image reprinted from ref. [6] with permission from Elsevier. (b) Cross section of functionally*
 92 *graded coating with interlayer tungsten content indicated.*

93 Regarding the optimum thickness of the FGM, a number of different FGM thicknesses was modelled for a
 94 finite element simulation covering several hundred operational cycles of a fusion reactor [6]. With this
 95 simulation the accumulated creep strain within the coating was evaluated (Figure 1a), finding that a
 96 minimum FGM thickness of 1.2 mm is required for long-term coating performance [6]. This thickness has

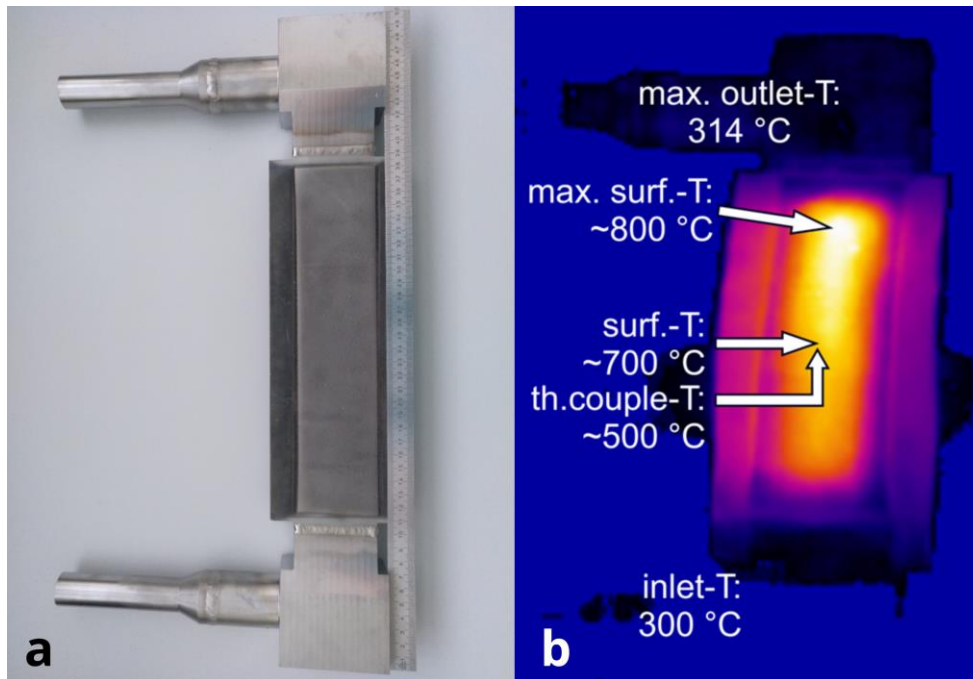
97 been used as design rationale for all following coating experiments, in order to achieve coatings as shown
98 in Figure 1b, with a 1.2 mm thick linearly graded FGM and a 0.8 mm thick W top layer realising the 2 mm
99 coating thickness specified for DEMO [7].

100 The promising performance results obtained during this early development phase sparked a drive towards
101 upscaling of this coating technology using the optimised parameters. Figure 2 shows an overview of
102 upscaled components coated up to now and includes an outlook towards current and future experiments to
103 transfer the coating technology from flat surfaces to fusion-relevant curvatures.



104
105 *Figure 2. Overview of different development steps during upscaling of coating technology.*

106 As a first upscaling step, several mock-ups of EUROFER steel were fabricated at KIT and coated at FZJ on
107 an area sizing up to 270×115 mm² (specimen on the left in Figure 2) [16]. One of these mock-ups (Figure
108 3a) was subjected to a high heat flux test (1000 cycles of 0.7 MW/m²) [16,25] in the Helium Loop Karlsruhe
109 (HELOKA) [26]. During the high heat flux test, surface temperatures of up to 800°C were measured (Figure
110 3b), but both coating and steel substrate remained undamaged [16].



111
 112 *Figure 3. (a) Mock-up with coated area 270x65 mm² for use in high heat flux test. (b) Infrared thermograph showing*
 113 *temperature of the mock-up during high heat flux test. Image reprinted and adapted from ref. [16] with permission from*
 114 *the IAEA and Euratom.*

115 After this promising outcome, further upscaling of the coated area was pursued which required a larger
 116 coating facility. For this, the knowledge of the FGM coating technology was transferred to the industrial
 117 company COATEC GmbH (Schlüchtern, Germany). As a result of this technology transfer, plates of P92
 118 steel which contain cooling channels were coated. P92 has similar non-irradiated thermo-mechanical
 119 properties as EUROFER steel but is more readily available [24]. Two of these plates with uniform coating
 120 are depicted in the middle of Figure 2, sizing 300x200 mm² and 500x250 mm², respectively. This technology
 121 transfer was successful, with good achievement of specified coating thickness, gradation and microstructure
 122 [24].

123 At this point, four potential fields for future research on these coatings may be identified:

- 124 (i) Further process development and upscaling of coated components. As of now, the above-
 125 mentioned steps pose the state of the art. Progress in this field, both in size and geometry of
 126 the coated components, is required in order to achieve technology readiness for the equipment
 127 of a full-size breeding blanket with the required tungsten protection.
- 128 (ii) Detailed characterisation of thermo-mechanical properties of the coating, taking mixing ratio
 129 and the heterogeneous microstructure into account. The coating's material properties are
 130 difficult to obtain by standard testing techniques, yet are required to enhance the predictive
 131 power of simulations of large scale coated components.
- 132 (iii) Hydrogen retention of the coating and its performance under plasma exposure. The issue of
 133 tritium fuel retention in a heterogeneous, porous microstructure was already discussed above.
 134 Furthermore, the alteration of the coating's surface should be investigated here.

135 (iv) Coating performance after neutron irradiation will remain an important point for future study,
136 even though irradiation-induced defects caused by displacements of lattice atoms (dpa) in steel
137 are expected to recombine and annealed out at the relatively high operating temperature of the
138 coating [27]. Tungsten, however, will not undergo such annealing at the given temperatures. In
139 addition, high-energy fusion neutrons would yield in both steel and tungsten transmutations
140 where the transmuted products, e.g. helium in steel and rhenium in tungsten, may form clusters,
141 bubbles [28] and even intermetallic precipitates [29] which would affect the thermo-physical and
142 thermo-mechanical properties of the coating. Hence, investigating the irradiation effects on the
143 FGM coating considering irradiation experiments among others in a fusion-oriented neutron
144 source like IFMIF-DONES is an important step towards its qualification.

145 This contribution sets a focus on the first of these four research fields. In the following sections, the coating
146 quality of the above-mentioned industry-coated plates is assessed further and a transfer towards coating of
147 curved surfaces is presented.

148 **3. Materials and methods**

149 **3.1 Further quality analysis of industry-coated plates**

150 The industry-coated plates sizing 300×200 mm² and 500×250 mm² were fabricated from P92 steel (1.4901)
151 and coated by vacuum/low pressure plasma spraying by the company COATEC GmbH as detailed in ref.
152 [24].

153 Non-destructive ultrasonic testing was conducted on the entire coated area of the plates to identify potential
154 weak spots. For this, a KC 200 Immersion testing facility was used, which included a USIP40 testing device
155 and KScan evaluation software (GE Inspection Technologies, Hürth, Germany). Details on the setup may
156 be found in [30].

157 From selected positions in the middle and corner of a 300×200 mm² plate (marked I and II in Figure 4a),
158 four-point bending specimens of dimensions 45×4×3 mm³ were cut by electric discharge machining, in order
159 to assess the quality of coating adhesion. The specimens consisted of steel substrate in their lower half and
160 coating in the upper half of the 4 mm dimension. In the middle of the 45 mm dimension, 1.5 mm deep and
161 approx. 0.1 mm wide notches were cut into the coating side by electric discharge machining to provoke
162 crack starting in the middle of the samples. Further notch sharpening and crack growth towards the coating-
163 substrate interface was achieved with a resonating fatigue machine (RUMUL CRACKTRONIC,
164 Russenberger Prüfmaschinen AG, Neuhausen am Rheinfall, Schweiz), applying an R-ratio of 0.1, a dynamic
165 load of 0.75 Nm and a change of the resonance frequency by -1.5 Hz as stop criterion indicating sufficient
166 crack growth at the notch tip.

167 Delamination of the coating was provoked by four-point bending the above-mentioned specimens in a
168 modified universal testing machine (Model 8062, INSTRON, Darmstadt, Germany) which additionally

169 included a vacuum high temperature furnace (MAYTEC Mess- und Regeltechnik GmbH, Singen, Germany).
170 The four-point bending was performed at fusion-relevant operation temperature of 550°C in vacuum (10^{-6}
171 to 10^{-3} mbar) using a displacement speed of 0.2 $\mu\text{m/s}$. The delaminated coating-substrate interface was cut
172 free by diamond wire cutting and examined by scanning electron microscopy (SEM, EVO MA10, Zeiss,
173 Oberkochen, Germany).

174 **3.2 Finite element analysis of curved substrate coating**

175 Transferring the developed coating technology from flat to curved substrates will lead to new residual stress
176 states in the curved coating. Finite element models of coated L-shaped specimens (Figure 5a) were
177 prepared to characterise the radial stress level to be expected at the coating-substrate interface when
178 coating a fusion-relevant curved surface. Three different models were compared, one with a coating over
179 the entire outer surface, one where only half of the curved segment is coated (the one shown in Figure 5a)
180 and one where only a quarter of the curved segment is coated. The comparison was done to assess whether
181 a partial coating is feasible since part of the curved segments in FW panels will be shadowed by
182 neighbouring panels so that a coating there is not necessarily required. The simulations were run with
183 ABAQUS, using a mesh of 4-node, bilinear generalised plane strain elements (ABAQUS: CPEG-4). The
184 use of generalised plane strain conditions is justified because in current First Wall designs the out-of-plane
185 dimension is very long (several metres) without significant change of the in-plane geometry. The smallest
186 mesh dimension (40 μm) was applied around the coating-substrate interface. Material properties for the
187 FGM interlayers were linearly interpolated between those of pure tungsten and EUROFER [6]. Elastic-ideal
188 plastic material behaviour was simulated. Fixed and loose bearing boundary conditions were applied to the
189 two straight ends, respectively. The cooldown process of a coated part after the coating process was
190 simulated by allowing the models to cool from the stress free state at 750°C to 20°C, with homogeneous
191 temperature over the parts. The resulting radial residual stress component was evaluated at the coating-
192 substrate interface in the curved region to predict if critical stresses would occur that endanger the
193 successful bonding.

194 **3.3 Coating of substrates with curved surface**

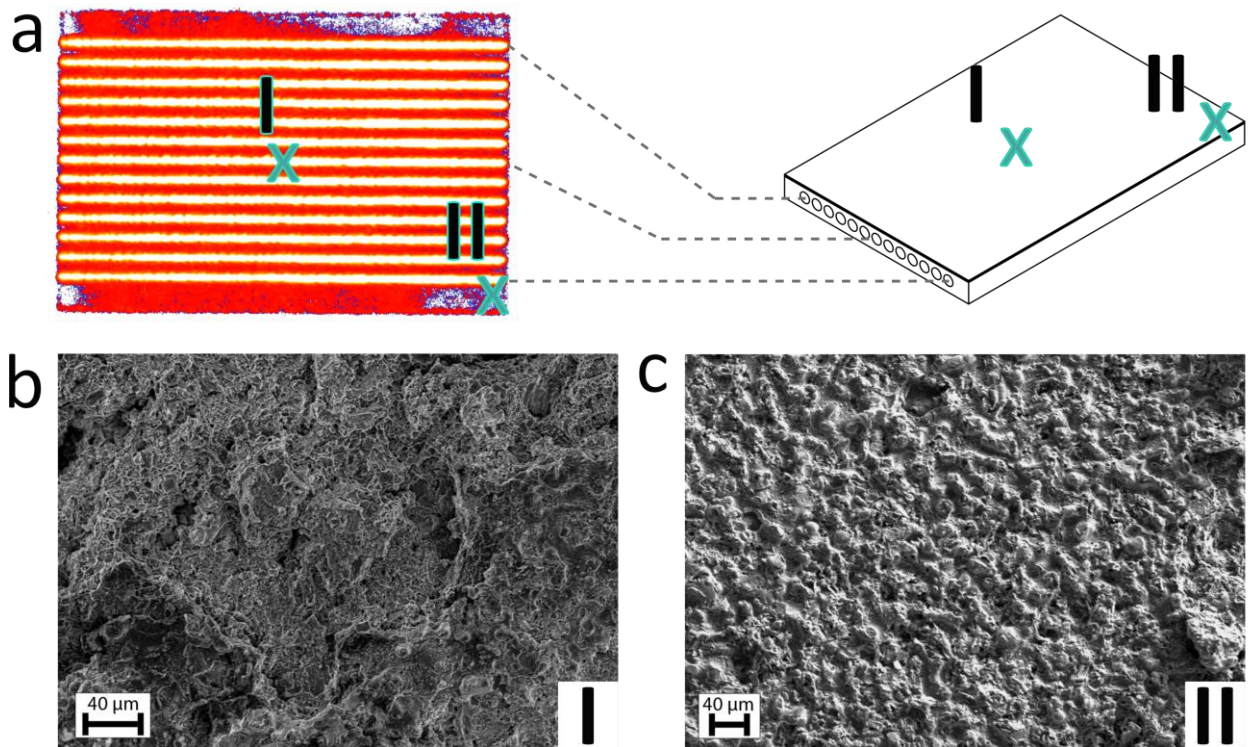
195 To test the feasibility of transferring the coating technology to convex curved substrates an L-shaped
196 specimen (Figure 6a) was prepared from P92 steel. The outer surface to be coated received a machined
197 finish and comprises two straight, flat sections as well as a central curved section with outer radius of
198 200 mm to match radii currently achievable in manufacturing of FW components [5,31]. The coating of this
199 outer surface was conducted at FZJ, similarly to previously published coating experiments and using powder
200 of similar grain size distribution [11,16]. However, the velocity of the spray process was reduced to 100 mm/s
201 on the flat segments to achieve comparable movement speeds in flat and curved regions, since the angular
202 velocity of the setup was limited. Two different coating procedures were tested, each on one half of the
203 specimen. For the first procedure, the spray process followed a vertical movement pattern as indicated by
204 the arrows in Figure 6a, for the second procedure it followed a horizontal pattern. For this pattern, a short

205 dwell time occurred while switching from rotational to linear movement. This led to a slightly larger coating
206 thickness at the transition area between straight and curved section. All other spray parameters were kept
207 constant. The substrates were preheated using the spray gun without powder feed. For this first feasibility
208 test, only a mixture of 50% W / 50% EUROFER was applied. The full FGM coating will be subject to a future
209 investigation. The quality of the coating was investigated by visual inspection and measurement of the
210 achieved coating thickness.

211 4. Results and discussion

212 4.1 Industry-coated plates: importance of temperature management

213 The result of the ultrasonic analysis of a 300x200 mm² plate is shown in Figure 4a, along with a schematic
214 of the plate for ease of understanding. The ultrasonic result depicts a C-scan, where red colour marks the
215 uncoated bottom side of the plate and the yellow/white horizontal stripes mark the cooling channels.
216 Blue/white colour in the corners of the plate marks potential weak spots within the coating, even though no
217 cracking was observed here and microstructure appeared similar to that in other regions. To scrutinise these
218 areas in more detail four-point bending specimens were cut out of a corner and out of the middle of the plate
219 for reference (positions marked I and II in Figure 4). The specimens were bent at 550°C in vacuum, to
220 provoke delamination under fusion-relevant conditions.



221
222 *Figure 4. (a) Ultrasonic analysis of coated 300x200 mm² plate and schematic illustration of plate. (b,c) Fracture surfaces*
223 *at coating-substrate interface after provoked delamination, samples from regions marked I, II in (a).*

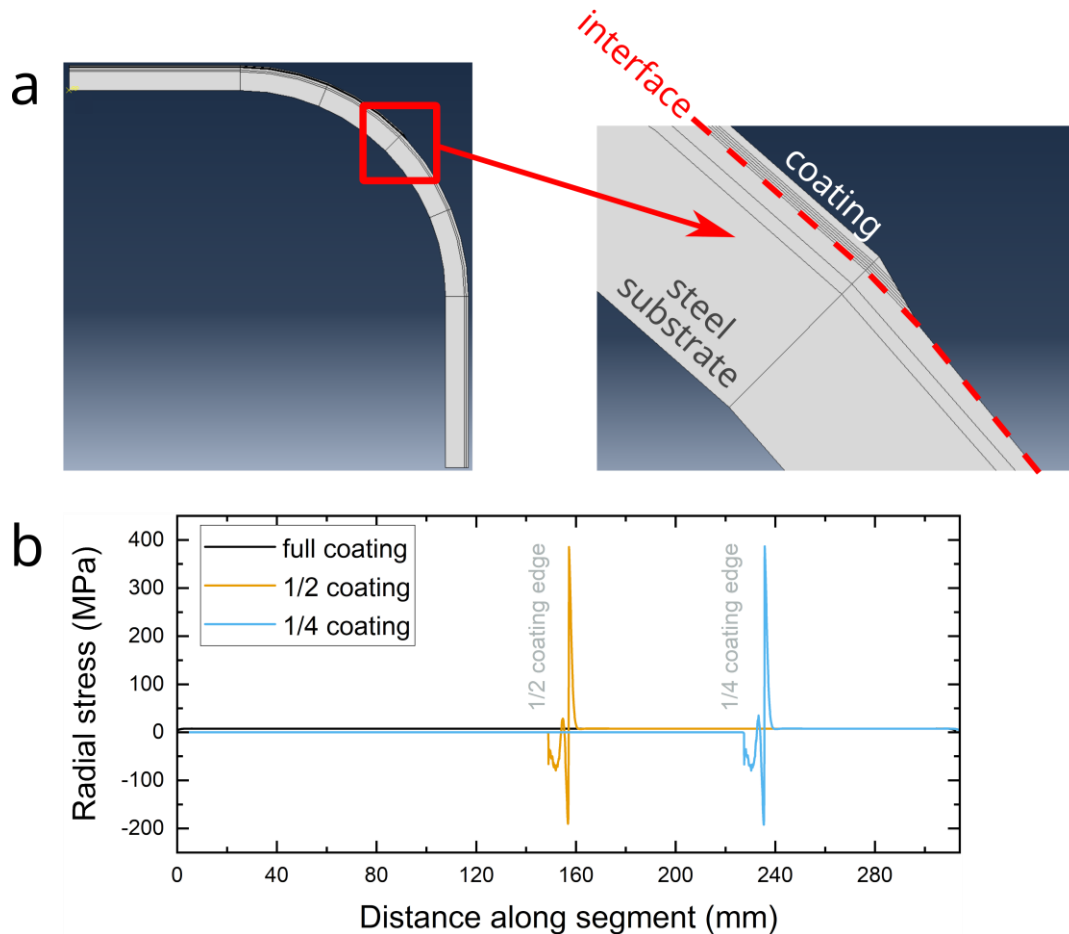
224 The delaminated surfaces at the coating-substrate interface were investigated with scanning electron
225 microscopy (Figure 4b,c). For the middle of the plate the delaminated surface showed a ridge pattern typical
226 for ductile fracture (Figure 4b), indicating good bonding between coating and substrate. For the corner of
227 the plate the fracture pattern indicated a brittle delamination (Figure 4c) and thus, potentially, insufficient
228 bonding. Such behaviour may be favoured by residual stress peaks in the coating close to the corners. The
229 combined results from ultrasonic testing and provoked delamination prove that the corners of this
230 investigated plate pose weak spots. The reason for the weak bonding between coating and substrate at the
231 corners may be found in the temperature distribution during the coating process. Here, the spray gun is the
232 only source of heat and moves back and forth over the plate, allowing some regions to cool down. In the
233 absence of countermeasures, the corners will then cool down faster than the rest of the plate. This was
234 verified with thermocouples as detailed in ref. [24]. Taken together, these results highlight the importance
235 of temperature management during the coating of larger components. With a sufficiently warm substrate
236 good bonding of the coating was achieved, but the temperature gradient over the coated area needs to be
237 minimised for a uniform coating quality. We note that the process could be optimised for coating 500×250
238 mm² plates. There, no more weak spots were detected during ultrasonic testing [24].

239 **4.2 Coating of curved surfaces**

240 All of the above-mentioned developments were performed on flat surfaces. Yet the design of First Wall
241 elements involves sections with a curved outer surface to be coated with tungsten [3]. The applicability of
242 the W/EUROFER FGM coating technology onto curved substrates thus needs to be proven. The curvature
243 can introduce out of plane stress components which can lead to delamination. Before testing the feasibility
244 of coating curved substrates in laboratory, a finite element analysis was therefore conducted in order to
245 assess the stress levels to be expected as well as potential critical spots. For the substrate, a simple L-
246 shaped geometry (Figure 5a) was modelled that involves a fusion-relevant outer radius of 200 mm as well
247 as two straight ends to model the transition from straight to curved sections. Three models were compared,
248 one being coated on the entire outer surface and two partial coatings that only cover one straight section
249 and half or a quarter of the curved section (named $\frac{1}{2}$ and $\frac{1}{4}$ coating). Even though a partial coating moves
250 the coating edge with its stress concentration into the critical curved section where additional out of plane
251 stress components occur, the $\frac{1}{2}$ and $\frac{1}{4}$ coatings were investigated to see whether the percentage of coated
252 curvature influences the stress underneath the coating. In a fusion reactor such as DEMO, parts of the
253 curved segments and sidearms of First Wall panels will be shadowed by neighbouring panels and thus do
254 not necessarily require a protective coating [32]. If partial coating of the curved segment is successful, the
255 shadowed regions may be omitted during coating. Besides material savings, this would save substantial
256 amounts of processing time considering the large amount of required First Wall panels, and may thus help
257 to reduce the cost of a reactor.

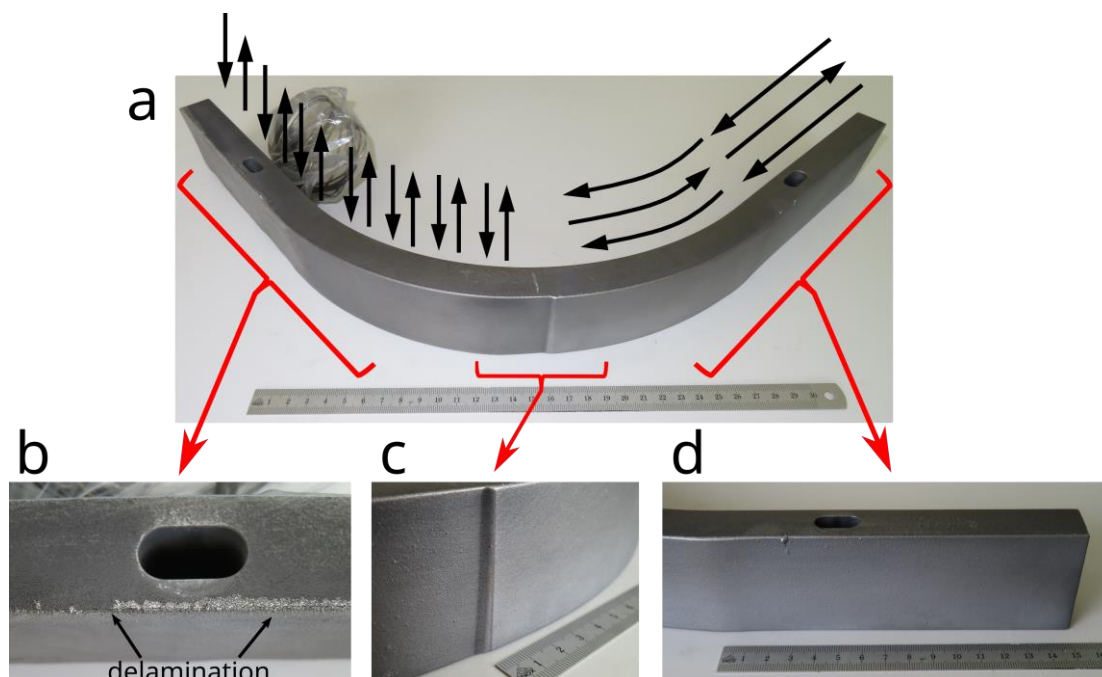
258 For this study the residual stress buildup after coating application was investigated by allowing the models
259 to cool down from stress free state at 750°C to 20°C. The radial residual stresses at the coating-substrate
260 interface were investigated (Figure 5b) since they are most critical for the stability of the coating. Since

261 ABAQUS provides poor interpolation of values at such interfaces, the analysed path was minimally shifted
 262 by one element's length (40 μm) into the steel substrate. The stress levels in Figure 5b are, however,
 263 representative, as was verified by continuous stress profiles perpendicular to this path (not shown here).
 264 Following Figure 5b from left to right along the length of the curved segment, the radial stresses are constant
 265 (approx. 8 MPa) for the fully coated model (black line). For the $\frac{1}{2}$ (orange) and $\frac{1}{4}$ coatings (blue) they start
 266 with zero stress on the uncoated surface, then passing a stress peak of about 400 MPa at the coating edge
 267 and then levelling down to a constant low value of about 8 MPa underneath the coating. This constant radial
 268 interface stress underneath the coating is identical for all three models, and its low value can be seen as
 269 uncritical for the performance of the coating. A stress discontinuity at the transition from curved to straight
 270 coating was minimal, i.e. a step from above-mentioned 8 MPa to zero radial stress. These results indicate
 271 that it does not matter how much of a curved section will be coated, the only critical point will be the stress
 272 concentration at the coating edge. This concentration will, however, also occur at the edge of a fully coated
 273 component and thus cannot be avoided. Whether such an edge actually leads to failure needs to be verified
 274 experimentally.



275
 276 *Figure 5. (a) Finite element model of a curved substrate with outer radius of 200 mm and coating over the top half of*
 277 *the outer surface (“ $\frac{1}{2}$ coating” in text). Magnification shows edge of coating. (b) Simulated radial stress at coating-*
 278 *substrate interface along curved segment with full / $\frac{1}{2}$ / $\frac{1}{4}$ coating. For the $\frac{1}{2}$ and $\frac{1}{4}$ coatings, the uncoated region is on*
 279 *the left (zero stress) and the coating begins towards the right, at the stress peaks.*

280 To test the feasibility of coating curved surfaces, L-shaped specimens were prepared to match the simulated
 281 geometry (Figure 6a). At the time of writing this contribution, only the first experiment was finished. The
 282 results presented in the following section thus need to be treated as preliminary, yet already allow for
 283 valuable insight. A single L-shaped specimen was coated at FZJ following two different procedures: One
 284 side was coated using a vertical up-down meander movement between specimen and spray gun (left side
 285 of Figure 6a, indicated by arrows). This movement was chosen to avoid a longer jump in coating thickness
 286 at the transition between straight and curved sections, when a translational movement of the sample holder
 287 needed to be switched to rotational movement. The other side was coated using a horizontal meander
 288 movement (right side of Figure 6a). For this first test, only a mixture of 50% W – 50% EUROFER was applied
 289 instead of the FGM. Coating thicknesses > 1 mm were achieved with both horizontal and vertical meander
 290 movements.



291
 292 *Figure 6. (a) Experimental coating on substrate with transition from straight to curved geometry, comparing vertical*
 293 *coating deposition (left, b) with horizontal deposition (right, d). Delamination was found near bearing for vertical*
 294 *direction (b). No delamination was found near coating tips in middle (c) or for horizontal coating direction (d).*

295 While for the vertical movement cracking and delamination of the coating was observed (Figure 6b), no
 296 defects were found in the middle of the sample where the two coatings ended in steps (Figure 6c). In Figure
 297 6c only the edge of the right coating is clearly visible since the edge of the left coating had a lower angle
 298 towards the substrate. The absence of cracking here indicates that a partial coating with edge may be
 299 created successfully despite the expected stress concentration at the edge (Figure 5b). The delamination
 300 observed on the experiment with vertical meander movement was most pronounced in the vicinity of the
 301 bearing hole (Figure 6b) where the sample was connected to a metallic sample holder. At this position the
 302 sample may quickly lose heat during the coating experiment. It is thus assumed that this region became too
 303 cold for successful bonding of the coating, similar to the above case of the corners of the flat 300x200 mm²

304 plate (Figure 4). For the horizontal meander movement, on the other hand, no cracking or delamination was
305 found. Here a sound coating was achieved (Figure 6d), its only discontinuity being a higher thickness at the
306 transition between straight and curved section (left end of Figure 6d) that could not be avoided here because
307 of a switching delay between translational and rotational movement. The absence of delamination here
308 indicates that the horizontal movement approach lead to a more homogeneous temperature distribution
309 over the coated area, thus avoiding formation of weak spots. This successfully applied coating with a transfer
310 from straight to curved substrate is a promising outcome for the first feasibility test. The remaining
311 experiments to be conducted will aim for applying the entire coating with FGM and to further improve
312 temperature management, so that a full coating can be applied onto curved segments in the future.

313 **5. Conclusions**

314 Joining tungsten and steel is a challenge in materials technology. The specifications for the future fusion
315 reactor DEMO call for even more: a stable, thick coating of tungsten on steel that needs to be applied over
316 areas in the square metres range and that needs to withstand substantial heat loads. Nevertheless, a
317 suitable coating technology was developed over the past years. This contribution summarises the major
318 development steps, ranging from early laboratory coating experiments via mock-ups for high heat flux tests
319 towards a technology transfer to industry in order to achieve upscaling of the coated area. The design
320 process was enhanced by combining findings from finite element simulation, processing and
321 characterisation to allow for quick identification of optimised parameters. Temperature management was
322 identified as an additional challenge when upscaling the components to be coated. Moreover, future first
323 wall panels will involve curved surfaces that need to be coated. The feasibility of coatings on fusion-relevant
324 curvatures was demonstrated here, both by simulating the expected stress levels and by running a first
325 feasibility test in laboratory. Future coating experiments for the First Wall of DEMO may build upon the
326 experience collected here in order to fully master the coating of curved surfaces and to drive the coated
327 area towards the size needed in fusion.

328 **Conflicts of interest**

329 There are no conflicts of interest to declare.

330 **Acknowledgements**

331 The authors thank Karl-Heinz Rauwald and Ralf Laufs (both FZJ) for performing VPS coating
332 experiments.

333 This work has been carried out within the framework of the EUROfusion Consortium, funded by the
334 European Union via the Euratom Research and Training Programme (Grant Agreement No 101052200 —
335 EUROfusion). Views and opinions expressed are however those of the author(s) only and do not
336 necessarily reflect those of the European Union or the European Commission. Neither the European
337 Union nor the European Commission can be held responsible for them.

- 339 [1] R. Arredondo, K. Schmid, F. Subba, G.A. Spagnuolo, Preliminary estimates of tritium permeation and
340 retention in the first wall of DEMO due to ion bombardment, *Nucl. Mater. Energy.* 28 (2021) 101039.
341 <https://doi.org/10.1016/j.nme.2021.101039>.
- 342 [2] European Research Roadmap to the Realisation of Fusion Energy, EUROfusion Programme
343 Management Unit, ISBN 978-3-00-061152-0, (2018).
- 344 [3] F.A. Hernández, P. Pereslavitsev, G. Zhou, Q. Kang, S. D'Amico, H. Neuberger, L.V. Boccaccini, B.
345 Kiss, G. Nádasí, L. Maqueda, I. Cristescu, I. Moscato, I. Ricapito, F. Cismondi, Consolidated design of
346 the HCPB Breeding Blanket for the pre-Conceptual Design Phase of the EU DEMO and harmonization
347 with the ITER HCPB TBM program, *Fusion Eng. Des.* 157 (2020) 111614.
348 <https://doi.org/10.1016/j.fusengdes.2020.111614>.
- 349 [4] R. Lindau, A. Möslang, M. Rieth, M. Klimiankou, E. Materna-Morris, A. Alamo, A.-A. Tavassoli, C.
350 Cayron, A.-M. Lancha, P. Fernandez, N. Baluc, R. Schäublin, E. Diegele, G. Filacchioni, J. Rensman,
351 B. v. d. Schaaf, E. Lucon, W. Dietz, Present development status of EUROFER and ODS-EUROFER
352 for application in blanket concepts, *Fusion Eng. Des.* 75–79 (2005) 989–996.
353 <https://doi.org/10.1016/j.fusengdes.2005.06.186>.
- 354 [5] L. Forest, L. Boccaccini, L. Cogneau, A. Li Puma, H. Neuberger, S. Pascal, J. Rey, N. Thomas, J. TOsi,
355 M. Zmitko, Test blanket modules (ITER) and breeding blanket (DEMO): History of major fabrication
356 technologies development of HCLL and HCPB and status, *Fusion Eng. Des.* 154 (2020) 111493.
357 <https://doi.org/10.1016/j.fusengdes.2020.111493>.
- 358 [6] D. Qu, W. Basuki, J. Aktaa, Numerical assessment of functionally graded tungsten/EUROFER coating
359 system for first wall applications, *Fusion Eng. Des.* 98–99 (2015) 1389–1393.
360 <https://doi.org/10.1016/j.fusengdes.2015.06.120>.
- 361 [7] L.V. Boccaccini, L. Giancarli, G. Janeschitz, S. Hermsmeyer, Y. Poitevin, A. Cardella, E. Diegele,
362 Materials and design of the European DEMO blankets, *J. Nucl. Mater.* 329–333 (2004) 148–155.
363 <https://doi.org/10.1016/j.jnucmat.2004.04.125>.
- 364 [8] L.V. Boccaccini, G. Aiello, J. Aubert, C. Bachmann, T. Barrett, A.D. Nevo, D. Demange, L. Forest, F.
365 Hernandez, P. Norajitra, G. Porempovic, D. Rapisarda, P. Sardain, M. Utili, L. Vala, Objectives and
366 status of EUROfusion DEMO blanket studies, *Fusion Eng. Des.* 109–111 (2016) 1199–1206.
367 <https://doi.org/10.1016/j.fusengdes.2015.12.054>.
- 368 [9] S. Heuer, J. Matějček, M. Vilémová, M. Koller, K. Illkova, J. Veverka, T. Weber, G. Pintsuk, J. Coenen,
369 C. Linsmeier, Atmospheric plasma spraying of functionally graded steel / tungsten layers for the first
370 wall of future fusion reactors, *Surf. Coat. Technol.* 366 (2019) 170–178.
371 <https://doi.org/10.1016/j.surfcoat.2019.03.017>.
- 372 [10] T. Weber, Z. Zhou, D. Qu, J. Aktaa, Resistance sintering under ultra high pressure of
373 tungsten/EUROFER97 composites, *J. Nucl. Mater.* 414 (2011) 19–22.
374 <https://doi.org/10.1016/j.jnucmat.2011.04.024>.
- 375 [11] R. Vaßen, K.-H. Rauwald, O. Guillon, J. Aktaa, T. Weber, H. Back, D. Qu, J. Gibmeier, Vacuum plasma
376 spraying of functionally graded tungsten/EUROFER97 coatings for fusion applications, *Fusion Eng.*
377 *Des.* 133 (2018) 148–156. <https://doi.org/10.1016/j.fusengdes.2018.06.006>.
- 378 [12] T. Weber, M. Stüber, S. Ulrich, R. Vaßen, W. Basuki, J. Lohmiller, W. Sittel, J. Aktaa, Functionally
379 graded vacuum plasma sprayed and magnetron sputtered tungsten/EUROFER97 interlayers for joints
380 in helium-cooled divertor components, *J. Nucl. Mater.* 436 (2013) 29–39.
381 <https://doi.org/10.1016/j.jnucmat.2013.01.286>.
- 382 [13] W.W. Basuki, J. Aktaa, Investigation on the diffusion bonding of tungsten and EUROFER97, *J. Nucl.*
383 *Mater.* 417 (2011) 524–527. <https://doi.org/10.1016/j.jnucmat.2010.12.121>.
- 384 [14] D. Qu, W. Basuki, J. Gibmeier, R. Vaßen, J. Aktaa, Development Of Functionally Graded
385 Tungsten/Eurofer Coating System For First Wall Application, *Fusion Sci. Technol.* 68 (2015) 578–581.
386 <https://doi.org/10.13182/FST15-113>.
- 387 [15] D. Qu, Z. Zhou, J. Tan, J. Aktaa, Characterization of W/Fe functionally graded materials manufactured
388 by resistance sintering under ultra-high pressure, *Fusion Eng. Des.* 91 (2015) 21–24.
389 <https://doi.org/10.1016/j.fusengdes.2014.12.014>.
- 390 [16] T. Emmerich, D. Qu, B.-E. Ghidersa, M. Lux, J. Rey, R. Vaßen, J. Aktaa, Development progress of
391 coating first wall components with functionally graded W/EUROFER layers on laboratory scale, *Nucl.*
392 *Fusion.* 60 (2020) 126004. <https://doi.org/10.1088/1741-4326/aba336>.

- 393 [17] D. Qu, Development of functionally graded tungsten/EUROFER coating systems (PhD thesis),
394 Karlsruhe Institute of Technology, 2016. <https://doi.org/10.5445/IR/1000061922>.
- 395 [18] T. Emmerich, D. Qu, R. Vaßen, J. Aktaa, Development of W-coating with functionally graded
396 W/EUROFER-layers for protection of First-Wall materials, *Fusion Eng. Des.* 128 (2018) 58–67.
397 <https://doi.org/10.1016/j.fusengdes.2018.01.047>.
- 398 [19] D. Qu, E. Gaganidze, R. Vaßen, J. Aktaa, Determination of interface toughness of functionally graded
399 tungsten/EUROFER multilayer at 550 °C by analytical and experimental methods, *Eng. Fract. Mech.*
400 202 (2018) 487–499. <https://doi.org/10.1016/j.engfracmech.2018.09.016>.
- 401 [20] T. Emmerich, R. Vaßen, J. Aktaa, Thermal fatigue behavior of functionally graded W/EUROFER-layer
402 systems using a new test apparatus, *Fusion Eng. Des.* 154 (2020) 111550.
403 <https://doi.org/10.1016/j.fusengdes.2020.111550>.
- 404 [21] D. Qu, M. Wirtz, J. Linke, R. Vaßen, J. Aktaa, Thermo-mechanical response of FG tungsten/EUROFER
405 multilayer under high thermal loads, *J. Nucl. Mater.* 519 (2019) 137–144.
406 <https://doi.org/10.1016/j.jnucmat.2019.03.019>.
- 407 [22] T. Weber, J. Aktaa, Numerical assessment of functionally graded tungsten/steel joints for divertor
408 applications, *Fusion Eng. Des.* 86 (2011) 220–226. <https://doi.org/10.1016/j.fusengdes.2010.12.084>.
- 409 [23] P. Pereslavtsev, C. Bachmann, U. Fischer, Neutronic analyses of design issues affecting the tritium
410 breeding performance in different DEMO blanket concepts, *Fusion Eng. Des.* 109–111 (2016) 1207–
411 1211. <https://doi.org/10.1016/j.fusengdes.2015.12.053>.
- 412 [24] T. Grammes, T. Emmerich, J. Aktaa, W/EUROFER functionally graded coatings for plasma facing
413 components: Technology transfer to industry and upscaling, *Fusion Eng. Des.* 173 (2021) 112940.
414 <https://doi.org/10.1016/j.fusengdes.2021.112940>.
- 415 [25] B.-E. Ghidersa, A.A. Sena, M. Rieth, T. Emmerich, M. Lux, J. Aktaa, Experimental Investigation of EU-
416 DEMO Breeding Blanket First Wall Mock-Ups in Support of the Manufacturing and Material
417 Development Programmes, *Energies.* 14 (2021) 7580. <https://doi.org/10.3390/en14227580>.
- 418 [26] B.E. Ghidersa, M. Ionescu-Bujor, G. Janeschitz, Helium Loop Karlsruhe (HELOKA): A valuable tool for
419 testing and qualifying ITER components and their He cooling circuits, *Fusion Eng. Des.* 81 (2006) 1471–
420 1476. <https://doi.org/10.1016/j.fusengdes.2005.06.370>.
- 421 [27] A. Chauhan, Q. Yuan, C. Dethloff, E. Gaganidze, J. Aktaa, Post-irradiation annealing of neutron-
422 irradiated EUROFER97, *J. Nucl. Mater.* 548 (2021) 152863.
423 <https://doi.org/10.1016/j.jnucmat.2021.152863>.
- 424 [28] E. Gaganidze, J. Aktaa, Assessment of neutron irradiation effects on RAFM steels, *Fusion Eng. Des.*
425 88 (2013) 118–128. <https://doi.org/10.1016/j.fusengdes.2012.11.020>.
- 426 [29] T. Tanno, A. Hasegawa, M. Fujiwara, J.-C. He, S. Nogami, M. Satou, T. Shishido, K. Abe, Precipitation
427 of Solid Transmutation Elements in Irradiated Tungsten Alloys, *Mater. Trans.* (2008) 2259–2264.
428 <https://doi.org/10.2320/matertrans.MAW200821>.
- 429 [30] T. Martin, S. Knaak, Y. Zhong, J. Aktaa, Ultrasonic Testing on EUROFER Welded Joints for
430 Determination of the Minimum Detectable Flaw Size - KIT Scientific Reports 7543, ISSN 1869-9669,
431 Karlsruhe Institute of Technology, 2010.
- 432 [31] H. Neuberger, J. Rey, A. von der Weth, Francisco Hernandez, T. Martin, M. Zmitko, A. Felde, R.
433 Niewöhner, F. Krüger, Overview on ITER and DEMO blanket fabrication activities of the KIT INR and
434 related frameworks, *Fusion Eng. Des.* 96–97 (2015) 315–318.
435 <https://doi.org/10.1016/j.fusengdes.2015.06.174>.
- 436 [32] Z. Vizvary, W. Arter, T.R. Barrett, D. Calleja, M. Firdaouss, J. Gerardin, M. Kovari, F. Maviglia, M.L.
437 Richiusa, DEMO First Wall misalignment study, *Fusion Eng. Des.* 146 (2019) 2577–2580.
438 <https://doi.org/10.1016/j.fusengdes.2019.04.046>.
- 439